Hindawi
Shock and Vibration
Volume 2018, Article ID 6412841, 9 pages
https://doi.org/10.1155/2018/6412841

Research Article

Experimental Study on Seismic Dynamic Characteristics of Shallow-Bias Tunnel with a Small Space

Feifei Wang,[1,2] **Xueliang Jiang**,[1] **Jiayong Niu**,[1] **and Hui Yang**[1]

[1] *College of Civil Engineering, Central South University of Forestry and Technology, Changsha, Hunan 410004, China*
[2] *Changsha Institute of Mining Research Co., Ltd., Changsha, Hunan 410012, China*

Correspondence should be addressed to Xueliang Jiang; iamjxl@163.com

Received 5 September 2017; Revised 8 March 2018; Accepted 7 June 2018; Published 28 June 2018

Academic Editor: Ivo Caliò

In order to obtain the seismic dynamic characteristics of a shallow-bias tunnel with a small space, a series of large-scale shaking table model tests were carried out. The key technology of the test is introduced in detail, for example, similar ratios of model, test equipment, testing model box, testing model, sensor arrangement, seismic waves, and testing system. The results show that the first predominant frequency is similar between measuring points. However, the second predominant frequency is highly different between measuring points. The first and second predominant frequencies gradually decrease with the increasing of input PGA. The rock stratum can shield seismic wave in the high frequency band. The research results provide reference for similar tunnels.

1. Introduction

In recent years, with the development of Chinese Western Development and the construction of the Silk Roads, many tunnels will be constructed in the mountainous and earthquake-prone western area. The shallow-bias tunnel with a small space may be the best option due to the objective conditions of geological structure, environmental condition, and engineering cost. Moreover, the tunnel meets the requirements of special geological condition and line direction. Nowadays, the tunnel has been widely constructed in tunnel engineering practice.

Shaking table test is a kind of advanced and sophisticated method in the study of geotechnical earthquake. At present, some scholars have studied the dynamic response of tunnel by the shaking table model test [1–5]. The dynamic response of tunnels passing through faults and weak strata was analyzed [6, 7]. The dynamic response of lining and portal slope of tunnel portal section is studied [1, 8]. The dynamic response of immersed tunnel in sea and river is studied [9, 10]. Gao et al. [11] carried out the large-scale shaking table model test to study the seismic response of lining stress with different types of seismic wave, seismic intensity, and different buried depth. Moss and Crosariol [12] investigated the horizontal racking distortion in an immersed tunnel by using the shaking table tests. Compared to numerical analyses, the measured horizontal "racking" distortions of the tunnel suggest that current simplified design methods may overestimate distortions in soft-soil situations. Xu et al. [13] carried out a series of shaking table tests to investigate the mechanism and the effect of seismic measures of mountain tunnel. They found that the adding a layer of steel wire mesh, installing a geofoam isolation layer and flexible joints, and reinforcing surrounding rock could reduce the dynamic response of tunnel. Wang et al. [14] carried out a series of shaking table tests to study the effect of the seismic wave type, excitation directions, and peak acceleration on the acceleration and strain response characteristics of the tunnel. Jiang et al. [15] investigated seismic response characteristics of acceleration response, dynamic strain, and surrounding rock pressure of the tunnel by using the shaking table test. This paper deals with shaking table tests on a tunnel-soil system. Some scholars also carried out the research [16–20].

The study on acceleration, strain, and internal force response of conventional tunnel has achieved rich results from above-mentioned literatures. However, there are few studies on the Fourier spectra response and variation laws of predominant frequencies for the tunnel. The variation rule

Table 1: The similar constants.

Physical quantity	Similar relation	Similar constants
L(m)	C_l	10
ρ(kg·m^{-3})	$C_\rho = 1$	1
E(MPa)	$C_E = C_\rho \cdot C_l$	10
ε	$C_\varepsilon = 1$	1
σ(kPa)	$C_\sigma = C_\rho \cdot C_l$	10
μ	$C_\mu = 1$	1
t(s)	$C_t = C_l^{0.5}$	3.16
a(m·s^{-2})	$C_a = 1$	1
u(mm)	$C_u = C_l$	10
v(mm·s^{-1})	$C_v = C_l^{0.5}$	3.16
ω(Hz)	$C_w = C_l^{-0.5}$	1
φ(°)	$C_\varphi = 1$	1
γ(kN·m^{-3})	$C_\gamma = C_\rho$	1
C(kN·m^{-2})	$C_c = C_\rho \cdot C_l$	10

∗*L:* length, *ρ:* density, *E:* elastic modulus, *ε:* strain, *σ:* stress, *μ:* Poisson ratio, *T:* time, *a:* acceleration, *u:* displacement, *v:* velocity, *ω:* frequency, *φ:* angle of shear strength, *γ*: specific weight, and *C:* cohesion.

Table 2: Main parameters of shaking table.

Parameters	Specification
Platform size	4m×4m
Degree of freedom of motion	6Dofs in 3directions
Center distance of table-board	6-50m
Load capacity	30ton
Maximum displacement and acceleration	X:250mm, ±1.0g Y:250mm, ±1.0g Z:250mm, ±1.6g
Working frequency	0.1-50Hz
Maximum eccentricity moment	20 ton·m
Maximum overturning moment	30ton·m
Maximum seismic velocity	1000mm/s
Maximum vibration velocity of simple string	750mm/s

of the frequency of the measuring point can be obtained by Fourier spectrum response. And the response characteristics of the measuring point further can be obtained. The study on Fourier spectra and predominant frequencies was never carried out in [21]. A testing model of the tunnel was constructed in laboratory. And the large-scale shaking table model tests were carried out to obtain the response of Fourier spectra and the variation laws of predominant frequencies. The research results provide reference for similar tunnels.

2. Shaking Table Model Test

2.1. Similar Ratios of Model. This paper mainly adopted the method of [14, 21]. According to similarity theory, the parameters between testing model and prototype must satisfy similar relations. Under the actual conditions, the test parameters are difficult to satisfy the similar relationship. Therefore, some similar ratios are regarded as main parameters, such as geometry, acceleration, and density. Some factors of shaking table dimension, data acquisition system, bearing capacity, and model boundary effect are also considered in shaking table test. Other similar constants are obtained by similar theory and dimensional analysis method [22]. The similar constants of the model test are shown in Table 1.

2.2. Testing Equipment. The shaking table model tests were carried out in the National Engineering Laboratory of the High-Speed Railway Construction Technology of Central South University. The main parameters of shaking table are given in Table 2.

2.3. Model Box. Considering the size of shaking table, the rigid model box is independently designed and made. The model box has been widely used to carry out many shaking table tests of underground structure [23, 24]. The length, width, and height are 3.5 m (x), 1.5 m (y), and 2.1 m (z),

Table 3: Physical and mechanical parameters.

Materials	Material parameters				
	E (MPa)	μ	γ (kN·m^{-3})	Φ (°)	C (kPa)
Weakly weathered rock	6000	0.25	23	39	700
Weak rock	1300	0.3	20	27	200
Hard rock	18900	0.3	25	50	1500
Lining	34500	0.16	24	-	-

∗E: elastic modulus, μ: Poisson ratio, φ: angle of shear strength, C: cohesion, and γ: bulk density

Figure 1: Rigid model box.

Figure 2: Treatment of model boundary [21].

respectively. The model box structure must be strong without instability. The test results show that the model box will not resonate with the testing model. The model box is shown in Figure 1.

Before pouring the physical model of the tunnel, the boundary of the model box should be treated to reduce the error caused by the model box effect. There are three boundary treatment methods of model in shaking table test, such as sliding boundary, friction boundary, and flexible boundary [25, 26]. The sliding boundary is applied to the floor of the model box, which can prevent the relative slip. The flexible boundary is applied to inner wall of the model box in the axial direction of the tunnel, which can reduce constraint effect. The sliding boundary is applied to inner wall of the model box. The boundaries of the model box is shown in Figure 2, which refers to [21].

2.4. Physical Model and Layout of Transducers. The lining model is made of microconcrete. Galvanized iron wire is used to simulate steel fabric. The thickness of the lining is designed as 4cm. Each lining liner axial length is 0.5m. The abrasive tool is used to compose the prefabricated lining. According to multiple laboratory experiments, the better ratio of the lining model material is 1:6.9:1.3 (cement: sand: water). The steel mesh is used to simulate the mesh reinforcement in lining. After pouring the lining, it is maintained for 28 days in the natural state. The lining reaches a certain strength and the lining is placed in the model box. The lining mold is specially made to fabricate the linings (Figure 3(a)). The lining model is shown in Figure 3, which refers to [21].

There is a natural slope in the overlying strata of the tunnel. The slope gradient is 1:1.04. The testing model internal dimensions are 3.5m (length), 1.5m (width), and 1.8m (height), respectively. The surrounding rock of the tunnel is composed of weakly weathered rock, weak rock, and hard rock. The buried depth of the tunnel is 0.9m. The clear width of each hole is 0.7m. The thickness of the middle partition wall is 0.4m. The mortar is used to simulate the surrounding rock of the tunnel. The different strength mortar is used to simulate the different surrounding rock layers. The parameters of surrounding rock and lining material are given in Table 3. The physical model is shown in Figure 4.

The accelerometers are used in the experiment, which are used to measure the acceleration of tunnel lining. The type of accelerometer is 1221L-002. The measuring range is ±20m·s^{-2}. The sensitivity is 2000mv·g^{-1}. Five measuring points are designed at the arch foot, arch shoulder, and vault of the tunnel [27, 28]. The number of measuring points in left hole is from A1 to A5. The number is from A6 to A10 in right hole. The number is T0 on the table-board. Moreover, the layout of transducers is shown in Figure 4.

2.5. Seismic Wave and Loading System. The buildings and structures are subjected to the action of the complicated seismic wave, when the earthquake occurs. In shaking table test, bidirectional seismic wave is used as loading wave in

Figure 3: Mold and linings: (a) mold of lining; (b) prefabricated lining [21].

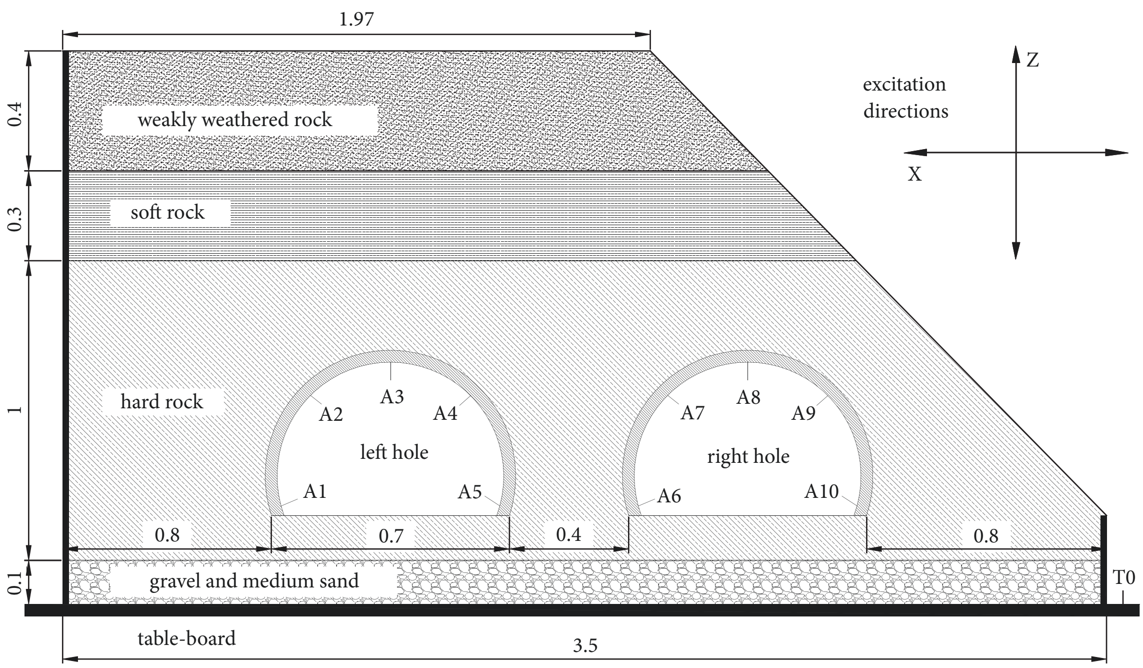

Figure 4: Surrounding rock and layout of transducers (unit: m).

order to get better simulation results. The bidirectional seismic wave is the Kobe wave (kb-xz). The horizontal direction (x) and vertical direction (z) are perpendicular to the tunnel axis, and table-board, respectively. The acceleration time history curve and the Fourier spectrum of the seismic wave are shown in Figure 5. The predominant frequency of Kobe wave is obtained by the Fourier spectrum, which is 4 Hz~ 13Hz. According to the code for seismic design of Chinese buildings (GB50011-2010), the vertical seismic waves are 2/3 times the peak of the horizontal seismic wave acceleration in the synthetic seismic waves of horizontal and vertical waves. According to the code for seismic design of Railway Engineering in China (GB50111-2006), the peak acceleration of seismic waves was adjusted to 0.1 g, 0.2 g, 0.4 g, and 0.6 g. In order to observe the dynamic characteristics of the test model, the white noise is loaded approximately 60S before each seismic wave loading. A total of 9 cases are arranged in the shaking table model test; the loading scheme is shown in Table 4.

3. Results of Tests and Analysis

3.1. Fourier Spectra Response. Case 1 is used to study the Fourier spectra response of different measuring points. Fourier transform is used to obtain Fourier spectrum of each measuring point, and the Fourier spectrum of each measuring point is showed in Figure 6. In order to easily obtain the predominant frequency in the curve of Fourier spectrum, the curve smoothing is used (Figure 6). The number in red rectangle is the measuring point corresponding to the Fourier spectrum in each picture.

In Figure 6, the first predominant frequency is 9.72Hz, and the second predominant frequency is 25.97Hz in each measuring point except A8 and A10. The characteristic periods 0.37s and 0.14s of the site are obtained from the similar constants. According to Code for Seismic Design of Buildings in China (GB50011-2010), the sites (0.37s and 0.14s) correspond to the II range and I_0 range, respectively. The component of first predominant frequency is basically

Table 4: Loading scheme of shaking table test.

Cases	Seismic wave	Peak acceleration	
		x-direction	z-direction
1	wn-xz	-	-
2	kb-xz	0.1g	0.067g
3	wn-xz	-	-
4	kb-xz	0.2g	0.133g
5	wn-xz	-	-
6	kb-xz	0.4g	0.267g
7	wn-xz	-	-
8	kb-xz	0.6g	0.400g
9	wn-xz	-	-

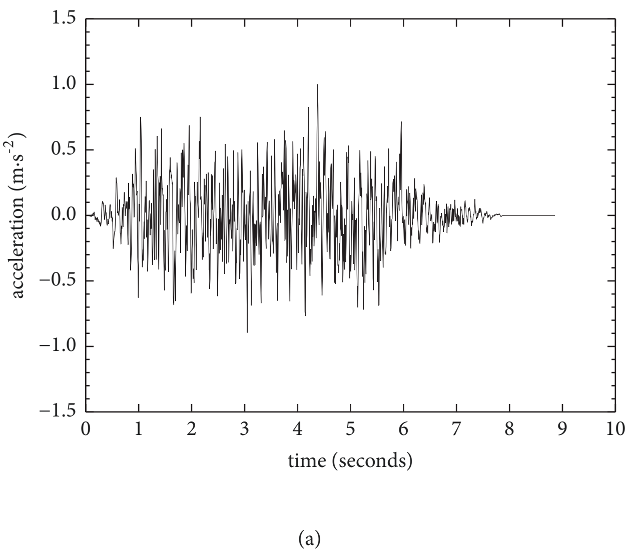

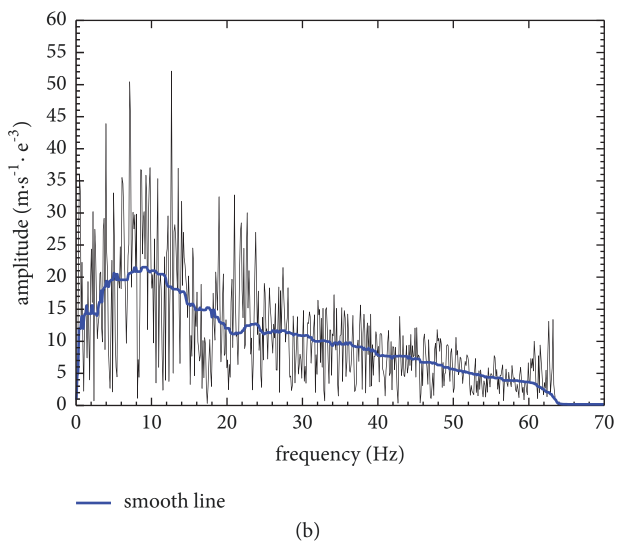

Figure 5: Kobe wave: (a) time history curve; (b) Fourier spectrum.

similar between measuring points. However, the second predominant frequency is different, some of the measuring points are amplified, and some of the measuring points are deamplified. The reason is that the first predominant frequency mainly reflects on the dynamic characteristics of the prototype site, but the second predominant frequency mainly reflects on the dynamic characteristics of the lining structure whose dynamic response is different with different measuring point [29]. By comparing the measuring points A1, A5, A6, and A10 on the same horizontal height, the high frequency is weakened, which illustrates the rock stratum can shield the seismic wave in the high frequency band of 20Hz-30Hz. Similarly, the law also is presented between A2, A4, and A7. The measuring point A9 is close to the slope, which has a significant influence on the seismic dynamic response of A9 and leads to the high frequency band of A9.

3.2. Predominant Frequencies. In order to obtain the effect caused by input PGA of seismic wave on the predominant frequency, cases 3, 5, 7, and 9 are used to study the dynamic response of measuring point 1. Fourier transform is also used to obtain Fourier spectrum of measuring point 1, and the Fourier spectra with different input PGA are showed in Figure 7. The variation of first and second predominant frequencies with the increasing of input PGA is given in Figure 8.

In Figure 8, the first and second predominant frequencies gradually decrease. The first predominant frequency decrease from 9.72Hz to 6.21Hz and decreases by 36.11%. The main reason is that, with the increasing of times loading and input PGA, the shear modulus of surrounding rock decreases continuously, and the 3.4 section can also verify the phenomenon. The second predominant frequency decreases from 25.97Hz to 22.11Hz and decreases by 14.86%. The reason for this phenomenon is that, after the seismic wave vibration, the cracks of the lining structure gradually develop, and the overall stiffness gradually decrease, resulting in the phenomenon of second predominant frequency decreasing.

4. Conclusion and Discussion

A physical test model of the tunnel was designed and manufactured to carry out a series of large-scale shaking table

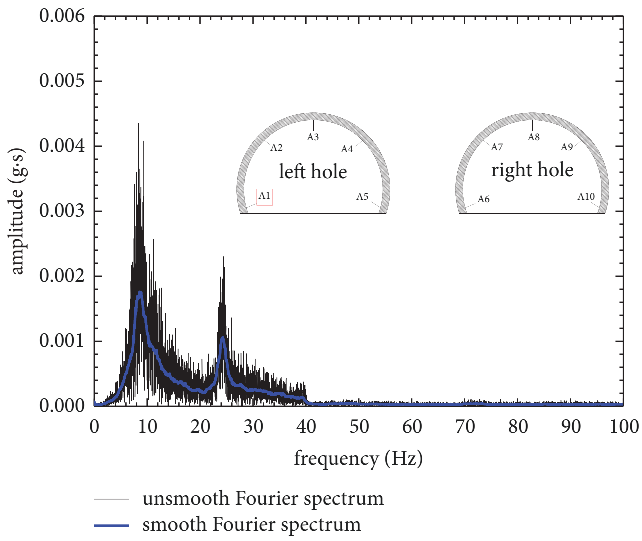

(a)

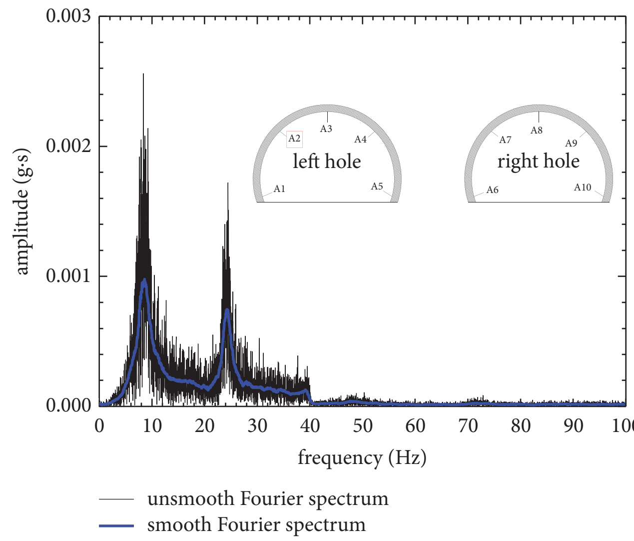

(b)

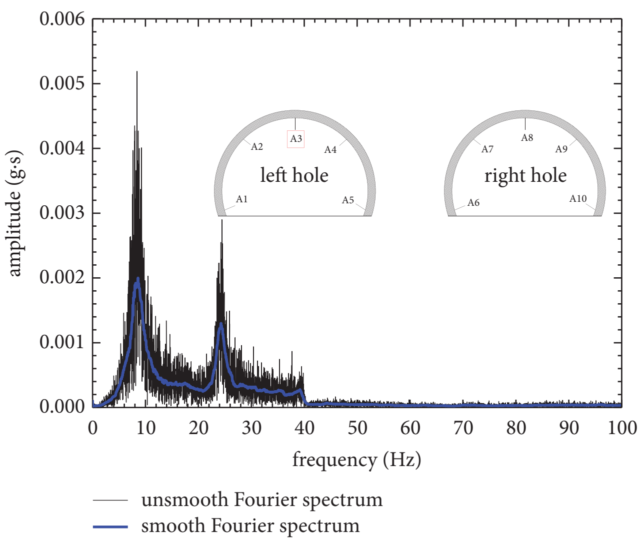

(c)

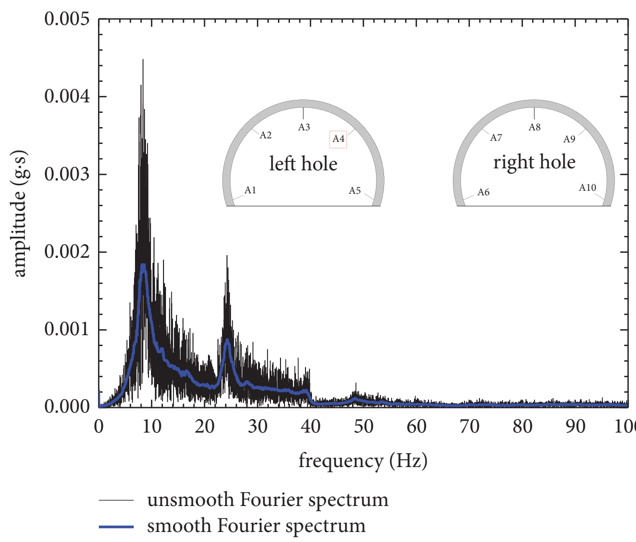

(d)

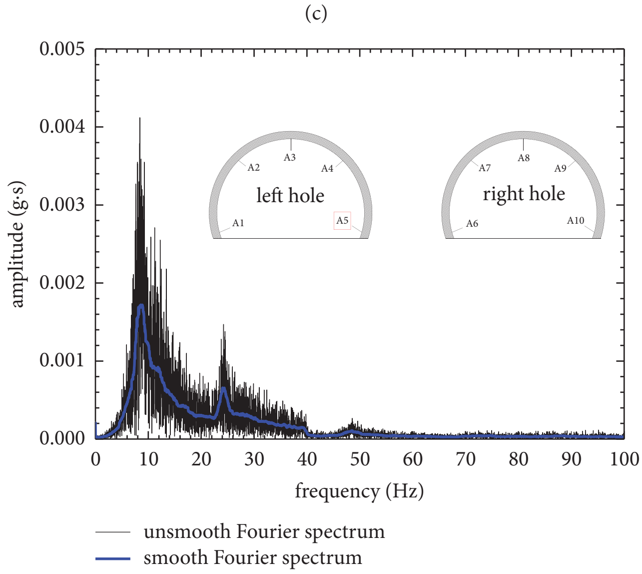

(e)

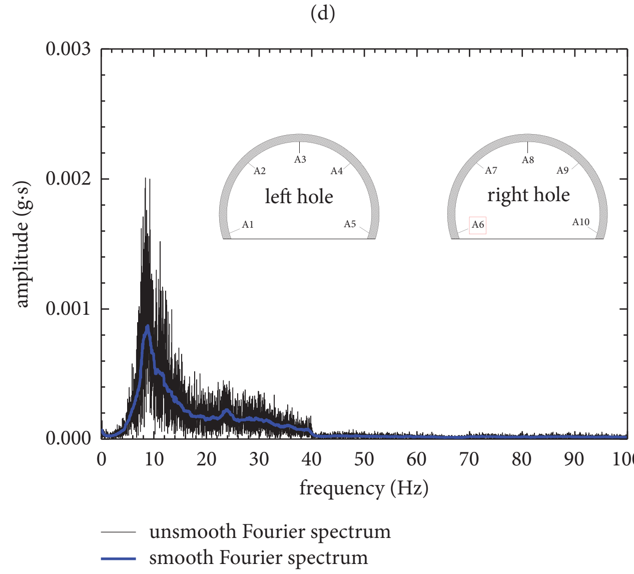

(f)

FIGURE 6: Continued.

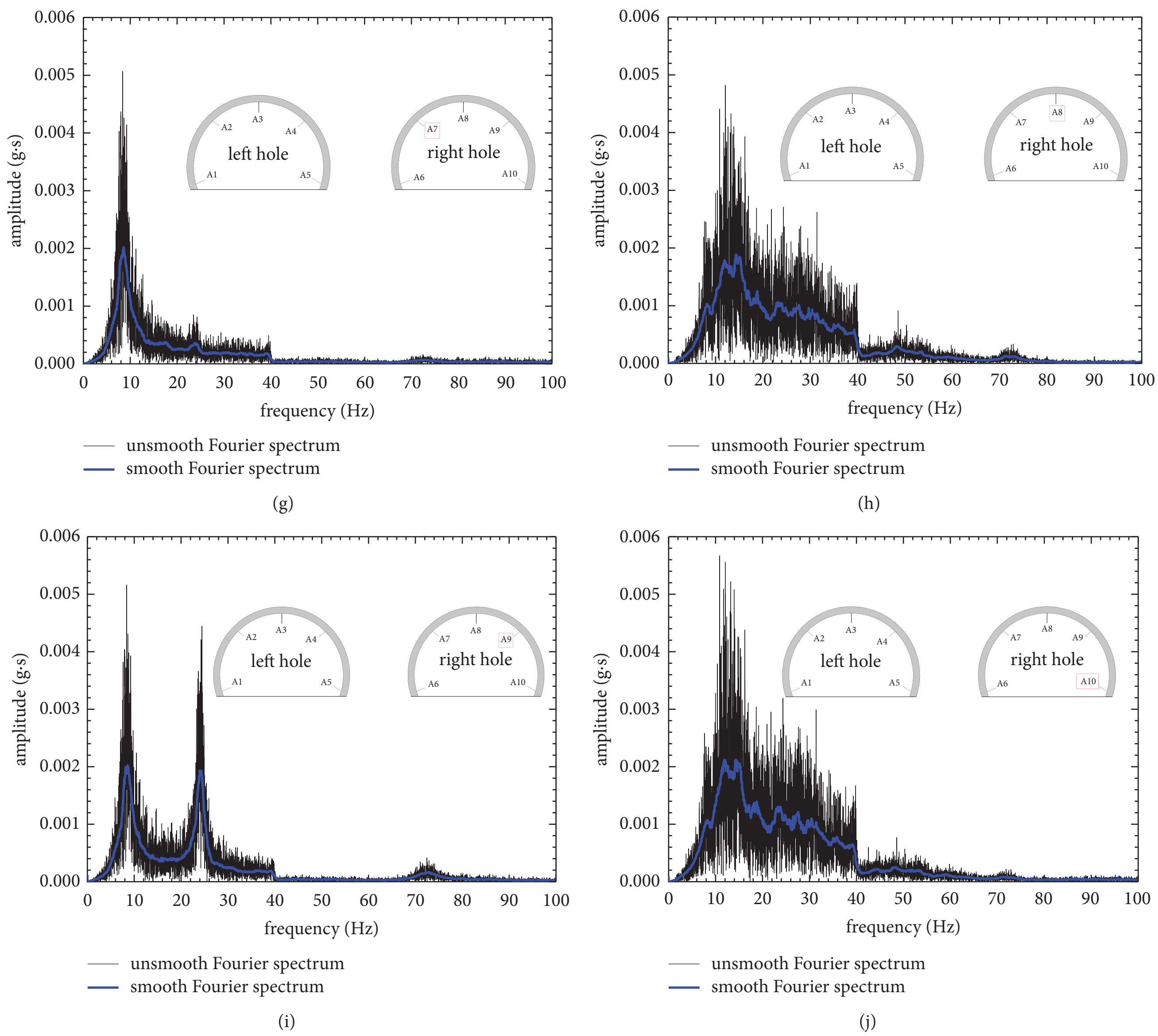

FIGURE 6: Fourier spectra of different measuring points: (a) measuring point A1; (b) measuring point A2; (c) measuring point A3; (d) measuring point A4; (e) measuring point A5; (f) measuring point A6; (g) measuring point A7; (h) measuring point A8; (i) measuring point A9; (j) measuring point A10.

model test. Based on the results of shaking table tests, the following conclusions can be drawn.

The first predominant frequency is 9.72Hz, and the second predominant frequency is 25.97Hz. The characteristic periods 0.37s and 0.14s of the site are obtained from the similar constants. The sites (0.37s and 0.14s) correspond to the II range and I_0 range, respectively.

The first predominant frequency is similar between measuring points. However, the second predominant frequency is different. The rock stratum and lining structure can shield the seismic wave in the high frequency band. The first and second predominant frequencies gradually decrease with the increasing of times loading and input PGA.

Conflicts of Interest

The authors declare that there are no conflicts of interest regarding the publication of this paper.

Acknowledgments

The research was supported from the National Natural Science Foundation (NNSF) of China (nos. 51204215, 51404309) and the Hunan Natural Science Foundation (no. 2018JJ3882). Finally, Feifei Wang wants to thank their supervisor, Professor Xueliang Jiang. Thank you for your meticulous teaching and careful cultivation in the past three years.

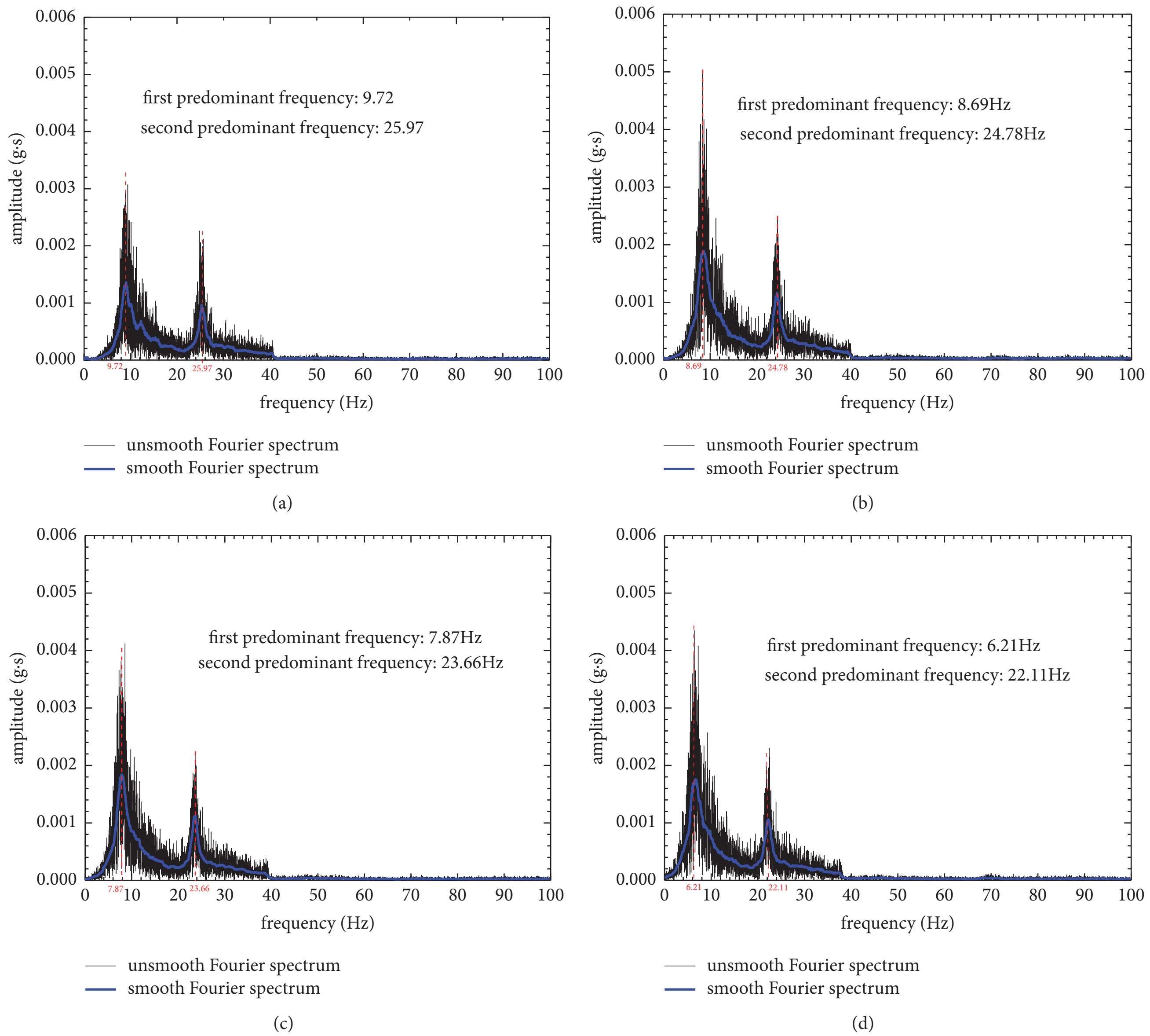

Figure 7: Predominant frequencies: (a) 0.1g; (b) 0.2g; (c) 0.4g; (d) 0.6g.

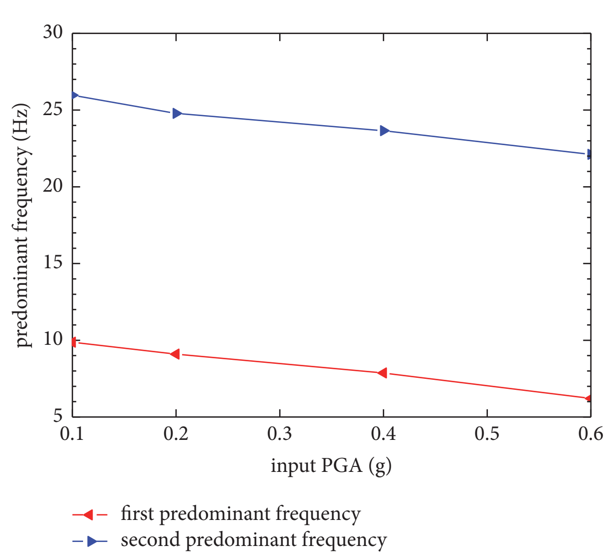

Figure 8: Predominant frequencies with input PGA.

References

[1] T. Sun, Z. Yue, B. Gao, Q. Li, and Y. Zhang, "Model test study on the dynamic response of the portal section of two parallel tunnels in a seismically active area," *Tunnelling and Underground Space Technology*, vol. 26, no. 2, pp. 391–397, 2011.

[2] J. Chen, X. Shi, and J. Li, "Shaking table test of utility tunnel under non-uniform earthquake wave excitation," *Soil Dynamics and Earthquake Engineering*, vol. 30, no. 11, pp. 1400–1416, 2010.

[3] S. Kiryu, Y. Murono, and H. Morikawa, "Seismic response of a cut-and-cover tunnel isolated by polymer material," *Earthquake Engineering & Structural Dynamics*, vol. 41, no. 14, pp. 2043–2057, 2012.

[4] Z. Z. Wang, Y.-J. Jiang, C. A. Zhu, and T. C. Sun, "Shaking table tests of tunnel linings in progressive states of damage," *Tunnelling and Underground Space Technology*, vol. 50, pp. 109–117, 2015.

[5] M. Rabeti Moghadam and M. H. Baziar, "Seismic ground motion amplification pattern induced by a subway tunnel: Shaking table testing and numerical simulation," *Soil Dynamics and Earthquake Engineering*, vol. 83, pp. 81–97, 2016.

[6] C. Xin L, B. Gao, and G. M. Yan, "Seismic damage characteristics and anti-seismic damping measures for tunnel across strike-slip faults," *Journal of Vibration Engineering*, vol. 29, no. 4, pp. 694–703, 2016.

[7] L. Fang, S. Jiang P, and Z. Lin, "Shaking table model test study of tunnel through fault," *Rock and Soil Mechanics*, vol. 32, no. 9, pp. 2709–2715, 2011.

[8] Z. Z. Wang, B. Gao, and Y. J. Jiang, "Investigation and assessment on mountain tunnels and geotechnical damage after the Wenchuan earthquake," *Science China Technological Sciences*, vol. 52, no. 2, pp. 546–558, 2009.

[9] X. Yan, H. Yu, Y. Yuan, and J. Yuan, "Multi-point shaking table test of the free field under non-uniform earthquake excitation," *Soils and Foundations*, vol. 55, no. 5, pp. 985–1000, 2015.

[10] X. Yan, J. Yuan, H. Yu, A. Bobet, and Y. Yuan, "Multi-point shaking table test design for long tunnels under non-uniform seismic loading," *Tunnelling and Underground Space Technology*, vol. 59, pp. 114–126, 2016.

[11] F. Gao, C. X. Sun, and X. K. Tan, "Different buried depth of seismic response of the tunnel shaking table test," *Rock and Soil Mechanics*, vol. 4, no. 9, pp. 2517–2531, 2015.

[12] R. E. S. Moss and V. A. Crosariol, "Scale Model shake table testing of an underground tunnel cross section in soft clay," *Earthquake Spectra*, vol. 29, no. 4, pp. 1413–1440, 2013.

[13] H. Xu, T. Li, L. Xia, J. X. Zhao, and D. Wang, "Shaking table tests on seismic measures of a model mountain tunnel," *Tunnelling and Underground Space Technology*, vol. 60, pp. 197–209, 2016.

[14] F. Wang, X. Jiang, and J. Niu, "The Large-Scale Shaking Table Model Test of the Shallow-Bias Tunnel with a Small Clear Distance," *Geotechnical and Geological Engineering*, vol. 35, no. 3, pp. 1093–1110, 2017.

[15] X. L. Jiang, J. Chen, and H. Yang, "Study on seismic response characteristics of unsymmetrically loaded tunnel based on large-scale shaking table test," *Journal of Nature Disasters*, vol. 25, no. 5, pp. 158–166, 2016.

[16] E. Bilotta, G. Lanzano, S. P. G. Madabhushi, and F. Silvestri, "A numerical Round Robin on tunnels under seismic actions," *Acta Geotechnica*, vol. 9, no. 4, pp. 563–579, 2014.

[17] G. Abate, M. R. Massimino, and M. Maugeri, "Numerical modelling of centrifuge tests on tunnel–soil systems," *Bulletin of Earthquake Engineering*, vol. 13, no. 7, pp. 1–25, 2015.

[18] G. Tsinidis, K. Pitilakis, and G. Madabhushi, "On the dynamic response of square tunnels in sand," *Engineering Structures*, vol. 125, pp. 419–437, 2016.

[19] G. Abate and M. R. Massimino, "Numerical modelling of the seismic response of a tunnel–soil–aboveground building system in Catania (Italy)," *Bulletin of Earthquake Engineering*, vol. 15, no. 1, pp. 469–491, 2017.

[20] G. Abate and M. R. Massimino, "Parametric analysis of the seismic response of coupled tunnel–soil–aboveground building systems by numerical modelling," *Bulletin of Earthquake Engineering*, vol. 15, no. 1, pp. 443–467, 2017.

[21] X. L. Jiang, F. F. Wang, H. Yang, G. C. Sun, and J. Y. Niu, "Dynamic response of shallow-buried small spacing tunnel with asymmetrical pressure: shaking table testing and numerical simulation," *Geotechnical and Geological Engineering*, pp. 1–19, 2018.

[22] P. J. Merymand, *Shaking table scale model tests of nonlinear soil-pile-super structure interaction in soft clay [Ph.D. thesis]*, University of California, Berkeley, Calif, USA, 1998.

[23] K. L. Fishman, J. B. Mander, and R. Richards Jr., "Laboratory study of seismic free-field response of sand," *Soil Dynamics and Earthquake Engineering*, vol. 14, no. 1, pp. 33–43, 1995.

[24] J.-S. Lee and J. C. Santamarina, "Seismic monitoring short-duration events: Liquefaction in 1g models," *Canadian Geotechnical Journal*, vol. 44, no. 6, pp. 659–672, 2007.

[25] D. Lombardi, S. Bhattacharya, F. Scarpa, and M. Bianchi, "Dynamic response of a geotechnical rigid model container with absorbing boundaries," *Soil Dynamics and Earthquake Engineering*, vol. 69, pp. 46–56, 2015.

[26] X. L. Jiang, F. F. Wang, H. Yang et al., "Dynamic response of shallow-buried tunnels under asymmetrical pressure distributions," *Journal of Testing and Evaluation*, vol. 46, no. 4, 2018.

[27] F. F. Wang, X. L. Jiang, H. Yang, P. Y. Lian, and J. Y. Niu, "Experiment and numerical simulation study on acceleration response laws of shallow-buried small spacing tunnel with asymmetrical pressure," *Journal of Vibration and Shock*, vol. 36, no. 17, pp. 238–247, 2017.

[28] X. L. Jiang, F. F. Wang, H. Yang, and J. Y. Niu, "Parameter sensitivity of shallow-bias tunnel with a clear distance located in rock," *Advances in Civil Engineering*, vol. 2018, 11 pages, 2018.

[29] Z. C. Guan, Z. F. Gong, and Z. B. Luo, "Seismic property of a large section tunnel based on shaking table model tests," *Rock and Soil Mechanics*, vol. 37, no. 9, pp. 2553–2560, 2016.